This article has been accepted for publication in a future issue of this journal, but has not been fully edited. Content may change prior to final publication. Citation information: DOI 10.1109/TIE.2017.2721878, IEEE Transactions on Industrial Electronics

Integrated Size and Energy Management Design of Battery Storage to Enhance Grid Integration of Large-scale PV Power Plants

Ye Yang, Qing Ye, *Student Member, IEEE*, Leonard J. Tung, *Michael Greenleaf, Member, IEEE*, Hui Li, *Senior Member, IEEE*

***Abstract*— Battery storage controlled by energy management system (EMS) becomes an enabling technique to enhance solar farm integration. In this paper, the EMS controls battery storage to shape the fluctuated PV plant output into a relatively constant power and support the peak load. The proposed integrated design method considers both battery size and EMS impacts on the utility benefits and cost. The utility benefits include power generation, peak power support, and reduced line losses. The cost of battery storage is determined by size and lifetime based on the developed battery models. Accordingly, the utility revenue change due to the battery storage controlled by EMS can be evaluated. Therefore, the integrated design of battery size and EMS can be determined by managing the change of utility revenue to gain economic benefits for the large-scale PV power plant application. Finally, the lithium-ion phosphate (LiFePO4) battery and lead-acid battery are compared to demonstrate the proposed method on a utility system model respectively.**

***Index Terms*— Battery storage, energy management system, large-scale PV plant, grid integration.**

NOMENCLATURE

EMS	Energy management system
P_{ref}	Power generation reference
P_{PPV}	PV peak power generation
d	Design parameter of EMS, the ratio of P_{ref} to P_{PPV}
P_{PG}	Battery power generation for peak load
E_B	Battery energy capacity
SOH	State of health
SOC	State of charge
DOD	Depth of discharge
$CL_{cyclation}$	Cyclation-based irreversible capacity loss
$CL_{calendrical}$	Calendrical-aging-based irreversible capacity loss
T	Nonoperation time
B_G	Benefit of annual energy generation
B_{PPG}	Benefit of annual peak power generation
B_{PL}	Benefit of annual power line losses reduction
C_B	Battery levelized cost
EP	Electricity price
$R_{curtail}$	Utility revenue based on curtailed PV generation
$Coulomb_{total}$	Total available coulomb under 100% DOD of an unused battery
$Coulomb_{used}$	Used coulomb of an battery
LC_{CT}	Levelized cost of gas combustion turbine
RP_{PL}	Reduced line losses
L_B	Battery lifetime
P_{Grid}	Power fed into the grid
P_{PG}	Battery power generation during peak load
P_B	Power of battery
P_{BMax}	Battery power rating

Manuscript received Aug., 2016; revised Dec., 2016, Feb., 2017, May, 2017; accepted Jun., 2017. This work was supported in part by. National Science Foundation under Grant ECCS-1001415 and the Department of Energy—Sunshine State Solar Grid Initiative (SUNGRIN) under Grant DE-EE0002063.

Ye Yang is with the National Institute of Clean-and-Low-Carbon Energy, Beijing, China (email: Yeyang.neo@live.com).

Michael Greenleaf is with the U.S. Nuclear Regulatory Commission, Atlanta, Georgia, USA (email: mike.c.greenleaf@gmail.com).

Qing Ye, Leonard J. Tung, and Hui Li are with the Department of Electrical and Computer Engineering, Florida State University, Tallahassee, FL. USA(e-mail: qye@caps.fsu.edu, tung@eng.fsu.edu, hli@caps.fsu.edu).

PCS	Power conditioning system
C_{PCS}	Unit cost of PCS
C_W	Unit cost of battery capacity
η	Battery power conversion efficiency
$CF_{install}$	Installation cost factor
N	Interest rate
FR	The annual power fluctuation rate
T	Temperature
$P_{Curtail\_PV_i}$	Curtailed PV generation
$FR_{Curtail}$	Annual power fluctuation rate when the PV output is curtailed
$FR_{Battery}$	Annual power fluctuation rate when the battery is deployed
L	Battery wire inductance in the leads
R_S	Battery cell ohmic contact and solution resistance
R_{OX}	Oxidation layer resistance formed at battery cathodes
C_{OX}	Oxidation layer capacitance formed at battery cathodes
R_{CT}	Charge transfer resistance formed at the electrolyte/electrode interface
C_{DL}	Effective double layer formed at the electrolyte/electrode interface
Z_W	Ionic diffusion through porous electrodes

I. Introduction

THE market for solar energy has been expanding rapidly worldwide, and the fastest growing sector within the solar market is the large-scale PV plant with outputs over 1 MW [1]. These grid-tied megawatt PV plants generally cause considerable power variation due to the weather conditions. The intermittent power generation of solar farms can perturb the supply and demand balance of the whole power system, and further cause stability issues such as voltage fluctuation and frequency variations [2]. Besides, the PV farms do not generate power at night, so they cannot support peak loads in residential applications. To maintain system frequency stability during the peak load period, spinning reserve is always adopted which inevitably increases system cost [3]. Recent research works have demonstrated that the battery storage can be used in PV farms to solve the above issues because of its flexible real power control [4-6]. Unfortunately, this technique has not been applied extensively, due to the high cost of batteries.

In order to achieve an effective and economical design of battery storage size, several research works have been developed [6-11]. In [6], the battery storage size is determined to maintain constant power production in PV plants according to the system requirement, however, the selected battery size has not been proved to be economical. A few battery sizing strategies have been developed by minimizing the investment on battery storage as well as the net purchased power for a residential or a commercial building with a rooftop PV system [7-11]. These methods are not suitable for large-scale PV plant applications, and the benefits to the utility company have not been detailed.

The battery EMS design has great impacts on the PV plant grid integration performance, which could affect the battery size selection as well. An energy management system (EMS) for PV power plants with energy storage was proposed in [12] to minimize the capacity requirement of energy storage, but no economic analysis was presented. In [13], an optimal power management strategy was presented for grid-connected PV systems with storage. The objective was to help intensive penetration of PV production into the grid by proposing peak shaving service at the lowest cost. Similarly, a price-based EMS was presented for roof-top PV installations with battery and local load [14]. The power output of the PV and battery systems are scheduled based on the time-varying price signals corresponding to the demand in the electricity networks. A co-optimization method for battery sizing and control strategy in a PV plant application was proposed in [15]. The operation and maintenance (O&M) cost and market penalties cost were considered. The proposed method in [15] has been applied in a PV plant. However, the system level related aspects such as annual power fluctuation rate of PV plant as well as the line power losses have not been analyzed. In addition, the preformation evaluation of different types of batteries has not been compared.

In this paper, an integrated approach to design the battery storage size and EMS for the grid-tied PV plant application is presented considering meeting system requirement and gaining economic benefits. The 1-minute interval PV plant output with load data from one utility company in Florida and the actual temperature data are applied to achieve more realistic results. EMS is developed to maintain the constant power generation and support peak load. The utility benefits including the improved power production, the peak power generation, and the reduced line losses are analyzed based on different battery size and EMS designs. The cost of battery storage is determined by the size and lifetime. As a result, the utility revenue change can be obtained under all possible battery sizes and EMS selections. Finally, an integrated design of battery size and EMS can be derived by managing the revenue to gain economic benefits using the method of exhaustion. The LiFePO4 battery and lead-acid battery are selected to demonstrate the proposed design method respectively due to the good performance of the former and the lower cost of the latter. Accordingly, by comparing the analysis results of these two batteries, the suitable battery type

This article has been accepted for publication in a future issue of this journal, but has not been fully edited. Content may change prior to final publication. Citation information: DOI 10.1109/TIE.2017.2721878, IEEE Transactions on Industrial Electronics

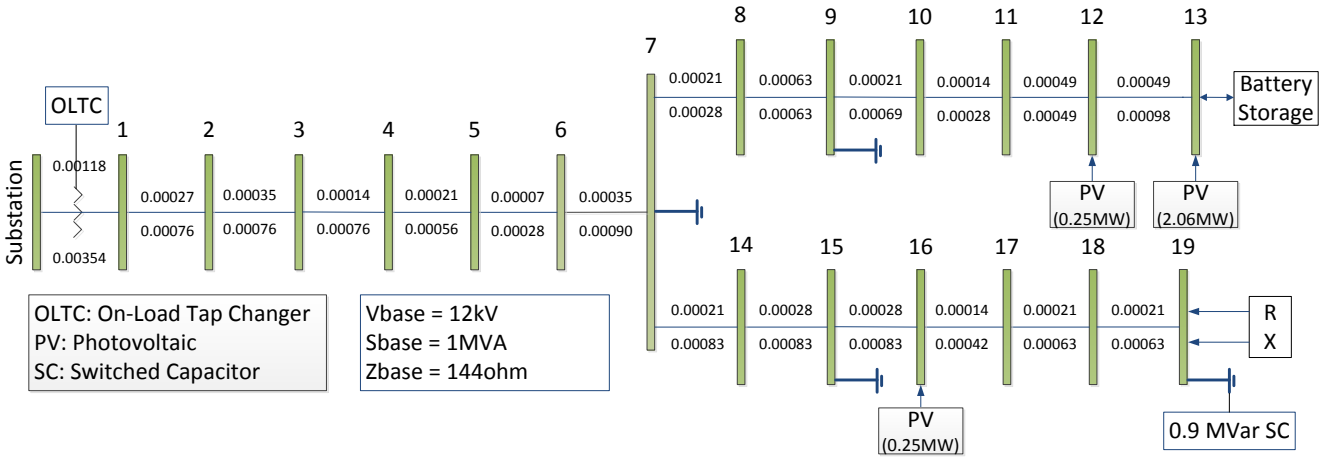

Fig.1. The utility system model.

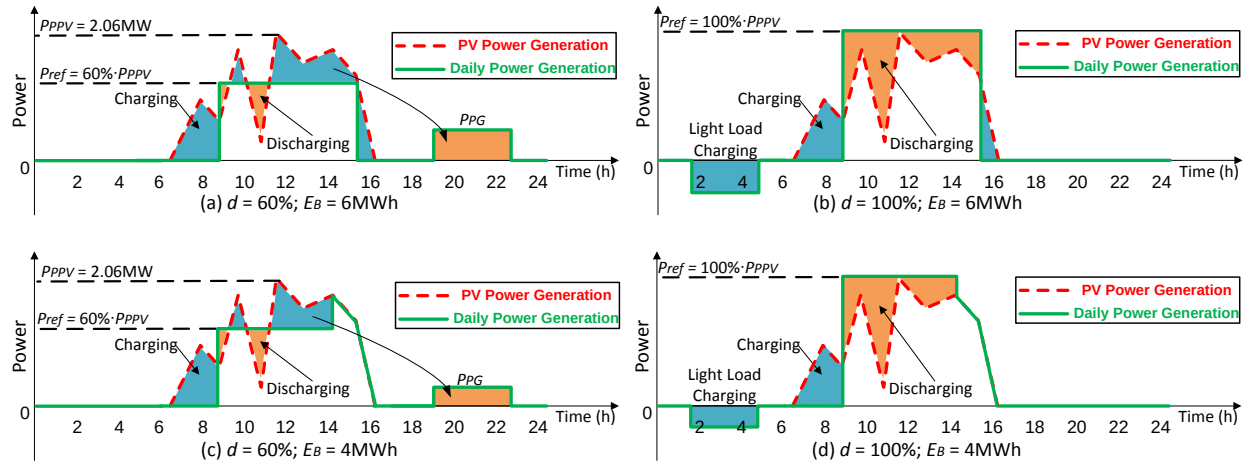

Fig. 2. The impact of E_B and d on daily generation.

for the PV plant applications can be identified as well.

II. System Description and Analysis

A. System description

In order to analyze the integrated impact of EMS and battery size for MW PV plant application, a utility system of Florida was selected. The simplified system model is shown in Fig. 1. It is an overhead 12 kV circuit for approximately 4.5 miles where the per-unit (p.u.) impedances of the transmission lines are labeled in the figure. The total system load is 11MVA. Since the customers of this utility are mostly residents, the peak load occurs between 7:00 p.m. – 11:00 p.m. The PV penetration level of this distribution system is close to 24% with one 2.06 MW PV plant connected to Bus 13 and two smaller PV systems connected to Bus 12 and Bus 16 at 0.25 MW and 0.35 MW respectively. The focus of this study is the 2.06 MW PV plant on Bus 13 with battery storage installed on the same bus. The objective of EMS is to control the battery storage to support this PV plant for a constant power production during the day time as well as to provide peak power generation during peak load at night. The design parameter of EMS is denoted as *d*, which is defined in (1):

$$d = \frac{P_{ref}}{P_{PPV}} \quad (1)$$

where P_{ref} is the desired plant power generation reference and P_{PPV} is the PV peak power which can be predicted one day ahead based on the weather forecast. *d* can be designed as any value from *0%* to *100%*.

B. Analysis of EMS and battery size on power generation

The PV plant daily generation performance is decided by both EMS and battery size. For example, if d = *60%* and a 6 MWh battery storage is installed in bus 13, the PV plant generation is depicted in Fig. 2(a). In this situation, the EMS will allow the battery to compensate P_{ref} and store extra energy at daytime (09:30 a.m. – 3:30 p.m.). Meanwhile, it will support peak load at night (7:00 p.m. – 11:00 p.m.) as long as its state of charge (SOC) is greater than 50%. If d increases to *100%*, the energy production during the daytime is increased shown in Fig. 2(b). Thus, the battery needs to discharge more and its SOC can drop down to 50%. As a result, the battery storage cannot support the peak load at night. However, if the battery energy capacity (E_B) is decreased to 4 MWh while the EMS remain the same, the PV plant output performances are

This article has been accepted for publication in a future issue of this journal, but has not been fully edited. Content may change prior to final publication. Citation information: DOI 10.1109/TIE.2017.2721878, IEEE Transactions on Industrial Electronics

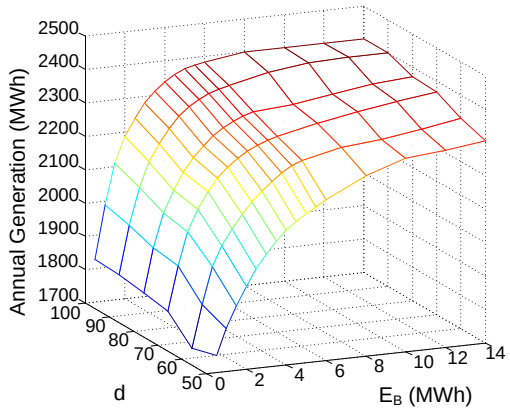

Fig. 3. The annual generation versus E_B and d on Bus 13.

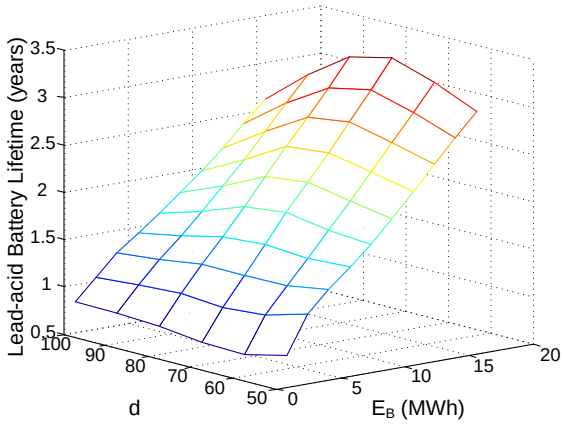

Fig. 4. The battery lifetime versus E_B and d on Bus 13.

different as shown in Fig. 2(c) and Fig. 2(d). When d = 60%, the 4 MWh battery will be charged to the upper SOC limit around 2:00 p.m. Then the plant output will follow the PV's output since the battery cannot limit the power fluctuation of PV plant. Accordingly, the stored energy in this battery becomes smaller than the one in Fig. 2(a), so does P_{PG}. Therefore, the battery storage has less capability to support peak load.

The simulated annual generation from PV and lead-acid battery storage of Bus 13 with different E_B and d is depicted in Fig. 3. It is noticed that, for a certain battery size E_B, EMS with higher d could increase the daytime power production, but the peak power generation of battery at night would be limited. For a certain d, a larger battery size would improve the daytime power generation and higher peak power generation capability. The analytical result is consistent with the analysis of Fig. 2. These two factors, i.e. EMS and battery size, need to be designed correlatively to meet the system requirement and achieve the cost-benefit solution.

C. The effect of EMS and battery size on battery lifetime

The EMS and battery size affect not only PV plant generation performance but also the battery lifetime. This can be observed briefly from Fig. 2 where a higher d will lead to more frequent discharge resulting in a shorter lifetime. In order to deplore the actual relationship of battery lifetime with E_B and d, SOH (the leftover lifetime of the battery in percentage) is calculated based on two major aging effects. One is the cyclation-based irreversible capacity loss ($CL_{\ cyclation}$), which represents the aging effect during normal discharge operation; the other is calendrical-aging-based irreversible capacity loss ($CL_{\ calendrical}$), which represents the aging effect during nonoperation time. These two aging effects and the lifetime of the battery can be derived in (2) to (4):

$$CL_{\ cyclation} = \frac{Coulomb_{used}}{Coulomb_{total}} \cdot 100\% \quad (2)$$

$$CL_{\ calendrical} = t \cdot Cal_{loss}(T, SOC) \cdot 100\% \quad (3)$$

$$SOH(\%) = 100\% - CL_{\ cyclation} - CL_{\ calendrical} \quad (4)$$

The total available coulomb ($Coulomb_{total}$) under 100% depth of discharge (DOD) of the unused battery can be estimated based on battery datasheet [16]. In practical operations, DOD normally was set lower than 100%, which would increase $Coulomb_{total}$. In this paper, the $Coulomb_{total}$ with 100% DOD was applied to emulate the worst-case scenario. The used coulomb ($Coulomb_{used}$) can be calculated according to the discharge power and time. Consequently, $CL_{\ cyclation}$ can be determined. Moreover, the calendrical irreversible capacity loss per day (Cal_{loss}) can be obtained based on the experimental results in [17], which vary under different temperature (T) and state of charge (SOC). Based on the nonoperation time (t), the $CL_{\ calendrical}$ can be calculated. The detailed method to determine $Coulomb_{total}$ and Cal_{loss} has been described in [11]. The initial value of SOH for an unused battery is 100%. With the increase of battery utilization and nonoperation time, the leftover lifetime SOH decreases. The battery will be scrapped when SOH reaches 0%; then the lifetime can be obtained. Based on (2) to (4), Fig. 4 demonstrates the calculated lifetime of battery of Bus 13 versus E_B and d.

III. Proposed Integrated Design Method

The previous analysis shows that both E_B and d can affect annual generation and battery lifetime, which are closely related to benefits and cost of the utility. Therefore, the objective function maximizes the utility revenue change to gain economic benefits in terms of E_B and d, which is formulated as follows:

$$\max_{E_B,\ d} \frac{B_G + B_{PPG} + B_{PL} - C_B - R_{Curtail}}{R_{Curtail}} \cdot 100\% \quad (5)$$

where B_G, B_{PPG} and B_{PL} are the annual benefits of the improved generation, peak power generation, and reduced line losses, respectively. C_B is the battery storage levelized cost. Traditionally, the output of a large-scale PV plant is curtailed to 50% of its maximum power generation in order to reduce the power fluctuation [18]. The profit of the curtailed PV generation ($R_{Curtail}$) is applied as the revenue baseline to evaluate the utility revenue change. The E_B and d, which

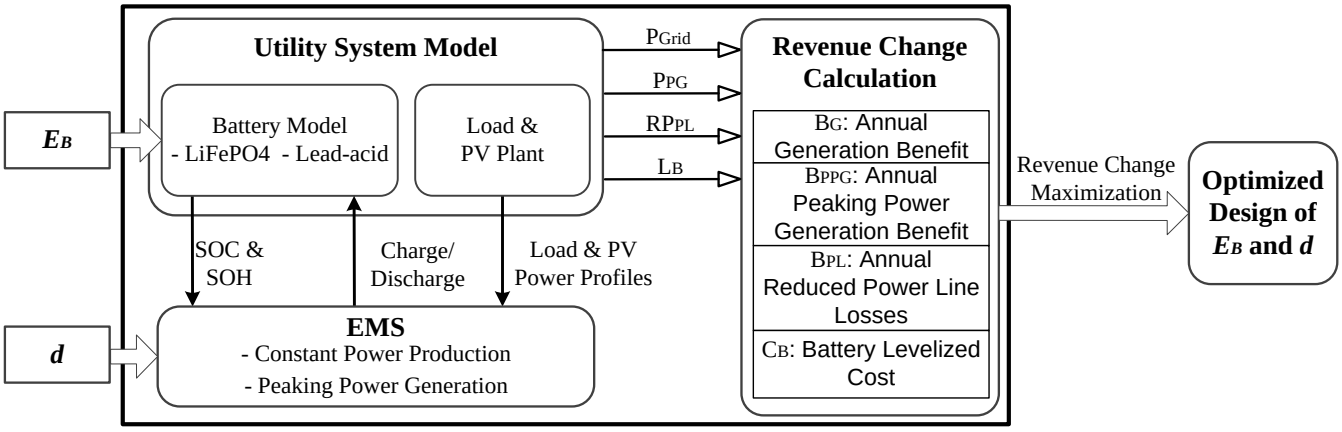

Fig. 5 The implementation block diagram of proposed integrated optimized design method.

decide the utility revenue change, will be considered as the desired battery size and EMS design. 1-minute resolution annual data was applied in the objective function (5) to find E_B and d for management of the utility revenue change.

$B_G, B_{PPG}, B_{PL}, C_B, R_{Curtail}$ can be derived in (6)-(10):

$$B_G = \sum_{i=1}^{n} EP_i \cdot P_{Grid\,i} \tag{6}$$

$$B_{PPG} = \frac{\sum_{i=1}^{n} P_{PG_i}}{m} \cdot LC_{CT} \tag{7}$$

$$B_{PL} = \sum_{i=1}^{n} EP_i \cdot RP_{PL_i} \tag{8}$$

$$C_B = \left(C_{PCS}P_{BMax} + \frac{C_W E_B}{\eta}\right)(1 + CF_{install})\frac{N(1+N)^{L_B}}{(1+N)^{L_B} - 1} \tag{9}$$

$$R_{Curtail} = \sum_{i=1}^{n} EP_i \cdot P_{Curtail\_PV_i}. \tag{10}$$

where EP_i is the electricity price. The time index in minutes is represented by i; n is equal to 525,600, the number of minutes in a year. $P_{Grid\,i}$ is the total power injected into the grid from bus 13. The value of B_G is positive if $P_{Grid\,i}$ is greater than zero, and vice versa. B_{PPG} represents the benefit of battery peak power generation. For generating the same amount of peak power, gas combustion turbine plant cost is reduced due to the unleashed power from battery storage during peak load time. P_{PG_i} is the battery power generation during peak load; m is the number of minutes for peak load time in a year, and LC_{CT} is the levelized annual cost of the gas combustion turbine [19]. B_{PL} is the benefit of the reduced line loss, where RP_{PL_i} is the reduced line losses depending on $P_{Grid\,i}$ and transmission line impedances. C_B is the annual levelized cost of battery that depends on the capacity rating(E_B) with its lifetime (L_B). The battery power conditioning system (PCS) cost is proportional to the battery power rating (P_{BMax}), which is same as P_{PPV}. C_{PCS} is the unit cost of the PCS. The cost of the storage is proportional to the battery capacity (E_B). C_W is the unit cost of the battery. η is the system efficiency [20]. The installation cost is proportional to the sum of PCS and storage cost [21]. As a result the installation cost factor $CF_{install}$ is introduced. N is the interest rate.

The objective function is subject to several constraints that are derived in (11)-(14).

Constraints:

$$P_{Grid_i} = P_{PV_i} + P_{B_i} + P_{Load_i} \tag{11}$$

$$P_{BMaxDischarge} \le P_{B_i} \le P_{BMaxCharge} \tag{12}$$

$$SOC_{Min} \le SOC_i \le SOC_{Max} \tag{13}$$

$$FR_{Battery} \le FR_{Curtail.} \tag{14}$$

The first constraint (11) maintains the power balance among the PV, the local load, the battery and the grid. P_{Gridi} is positive when the power is injected into grid from bus 13; P_{PVi} is positive if PV farm is generating power; P_{Bi} is positive if battery is discharging; P_{loadi} is negative if local loads are consuming power. Constraint (12) ensures that the charge/discharge power of the battery remains within the upper and lower bounds specified by the battery manufacturers. The third constraint (13) guarantees that the SOC is kept in the acceptable range. The annual power fluctuation rate (*FR*) is limited in (14). *FR* is the percentage of power fluctuation violation time in one year. Additionally, the power variation should be less than 40kW/min, as is defined in [18]. The power fluctuation rate when battery is deployed ($FR_{Battery}$) is desired to be comparable to the *FR* when PV output is curtailed ($FR_{Curtail}$).

The annual revenue change management procedure is summarized in Fig. 5. At first an initial E_B and d is provided to the battery model and EMS respectively. The SOC and SOH are derived from battery model and sent to EMS. In addition, the EMS also receives the load and PV power profiles from utility system model. Subsequently, EMS calculates the required charge/discharge power to meet the requirements in (11) and (14). Based on the present SOC and SOH, the power commands are limited based on constrains (12) and (13) before sending the command to battery model. Then the battery model updates its SOC and SOH for the next charge/discharge cycle. Finally, P_{Grid}, P_{PG}, RP_{PL}, and L_B can be obtained from utility system model for the benefits and cost calculation in (6)-(10) when the annual 1-minute interval PV, load, and temperature data are completely processed. As a result, the revenue change can be calculated using (5) for the given E_B and d. This process will be repeated until the final E_B and d found to achieve the maximized revenue change to gain economic benefits.

This article has been accepted for publication in a future issue of this journal, but has not been fully edited. Content may change prior to final publication. Citation information: DOI 10.1109/TIE.2017.2721878, IEEE Transactions on Industrial Electronics

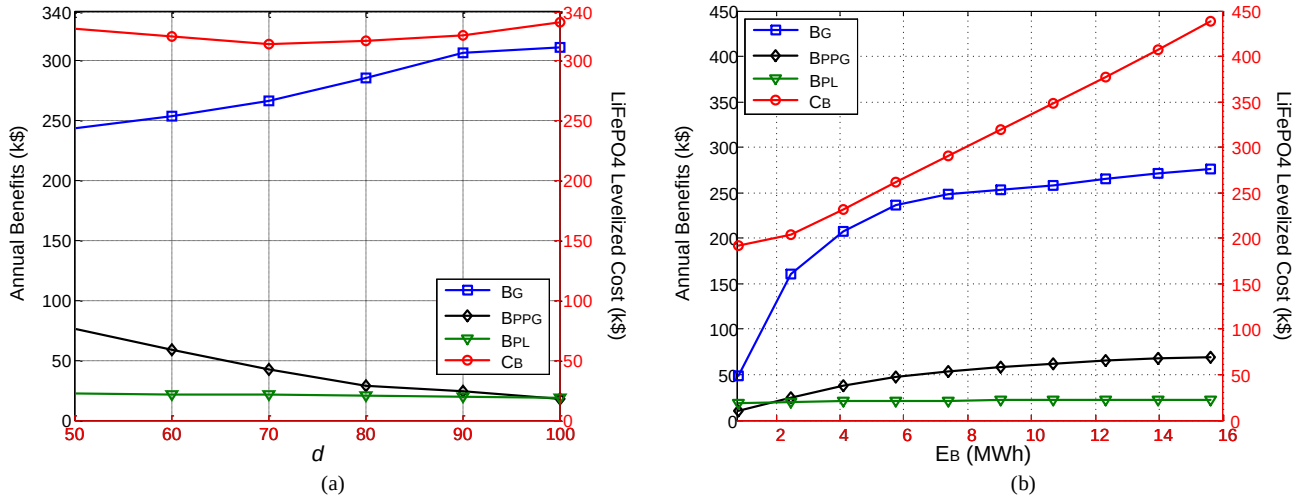

Fig. 6 Variation of B_G, B_{PPG}, B_{PL}, and C_B: (a) when d is varied and E_B = 9MWh; and (b) when E_B is a variable and d = 60%.

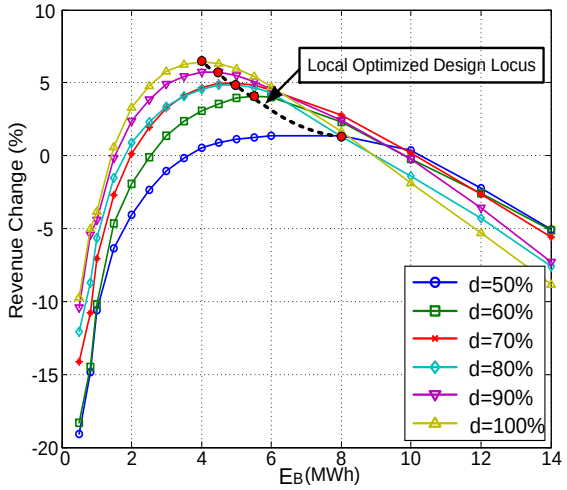

Fig. 7 The revenue change versus E_B and d.

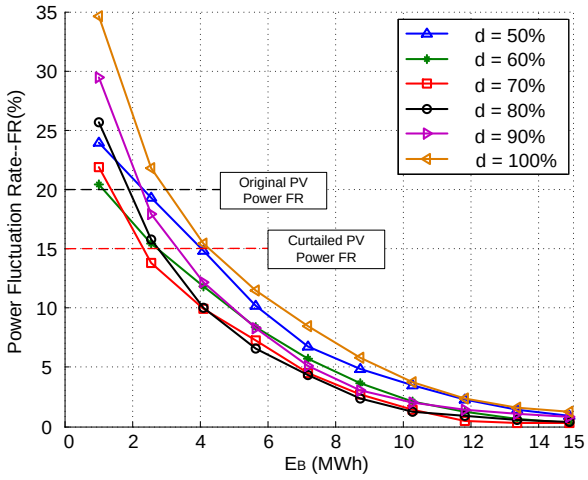

Fig. 8. Constraint evaluation: power fluctuation rate versus E_B and d.

IV. Results and Discussions

The proposed integrated design method has been applied to the Bus 13 of utility system model shown in Fig.1 where LiFePO4 battery system is adopted as energy storage. The range of E_B is selected from 0.5MWh ~ 15MWh and d is varied from 50% ~ 100%. The variation of B_G, B_{PPG}, B_{PL}, and C_B with d at any given E_B can be derived based on (6)-(10) and shown in Fig. 6(a) when E_B is selected as 9 MWh as an example. The analysis of session III illustrated that for a certain battery size E_B, higher d could increase the daytime power production, but the peak power generation of battery at night would be limited. The analysis is consistent with Fig. 6(a) where B_G is increasing and B_{PPG} is decreasing with d. The change of B_{PL} with d is small compared to other benefits, so it looks like a constant in Fig. 6(a). The C_B depends on the battery lifetime for a given E_B. A lower d will lead to more discharge operations during the night time, while a higher d cause more discharge during the day time, which accelerate the battery aging effect, therefore the lifetime of battery is smaller at both higher d and lower d (also shown from Fig. 4), leading to higher cost at both lower d and higher d. The variation of B_G, B_{PPG}, B_{PL}, and C_B with E_B at any given d can be derived similarly and shown in (b) when d is selected as 60% as an example. Although all the benefits and battery cost are increasing, but the slopes are different. Thus, there exists an optimal solution economically. Further, the revenue change versus E_B and d can be derived based on equation (5)-(10), and then plotted in Fig. 7. The global maximized revenue change can be found to be d=100% at E_B = 4MWh. The local highest revenue change for each d is derived and labeled as well. Similarly the local maximized revenue change for each E_B can be derived accordingly.

After the E_B and d are derived to achieve maximized economic benefit, it is important to evaluate the effect of proposed method on power fluctuation rate. In addition, the optimized design based on lead-acid battery will be compared with those of lithium-ion battery. The above aspects are discussed as follows.

This article has been accepted for publication in a future issue of this journal, but has not been fully edited. Content may change prior to final publication. Citation information: DOI 10.1109/TIE.2017.2721878, IEEE Transactions on Industrial Electronics

A. Effect of proposed design method on power fluctuation rate reduction

The design of E_B and *d* needs to be evaluated to analyze if it meets constrain (14), i.e., $FR_{Battery} \leq FR_{Curtail.}$ *FR* can be derived in (15):

$$FR = \frac{D_{|\Delta P|>40kw/min}}{D_{P>0}} \cdot 100\% \quad (15)$$

where $D_{\Delta P>40kw/min}$ is the time when the fluctuated power is violating the limit in one year, and $D_{P>0}$ is the annual generation time. Based on (15), *FR* of our target PV plant without energy storage is derived as 20%. A popular method of reducing *FR* is to curtail the output of the PV plant to 50% of its maximum power output, which was presented in [18]. Using the curtailed method, the $FR_{Curtail}$ of targeted PV plant is 15%. In this study, the objective of deploying battery storage with PV plant is not only achieving constant power generation but reducing *FR* as well. $FR_{Battery}$ of targeted PV plant with different E_B and *d* has been derived from simulation based on (15). As shown in Fig. 8, The *FR* reduces with the growth of the battery size E_B. The decreasing rate of *FR* has slowed significantly after 10MWh. Moreover, the range of E_B for every *d* designs which meet $FR_{Battery} \leq FR_{Curtail}$ can be found in this figure as well. For example, if *d = 50%* is selected, any E_B larger than 4MWh will allow $FR_{Battery} \leq$ 15%, which meets $FR_{Battery} \leq FR_{Curtail}$. In addition, Fig. 7 shows that when *d = 50%*, E_B = 8 MWh will achieve maximized revenue change, Fig. 8 shows that *FR* is 6% in this case which is less than $FR_{Curtail}$. Therefore it can be observed that all the derived E_B designs for certain *d* selection are satisfied constrain (11)-(14). Additionally, for certain E_B design, a proper *d* could be determined to achieve an acceptable *FR*. On the other hand, if a certain *d* is selected, E_B can be determined to reduce *FR* to certain levels as well.

B. Comparison of LiFePO4 battery-based design and lead-acid battery-based design

Fig. 6-8 show the design results of LiFePO4 battery working with targeted PV plant. The results of lead-acid battery can be derived similarly. The difference of designs between these two batteries is resulted from their models. Fig. 9(a) depicts the developed lead-acid battery model in this study. *L* represents wire inductance in the leads; R_S is the ohmic contact and solution resistances of the cell; R_{OX} and C_{OX} represent the resistance and capacitance of the oxidation layer formed on the cathode; R_{CT} and C_{DL} are charge transfer resistance and the effective double layer formed at the electrolyte/electrode interface; and Z_W represents the ionic diffusion through porous electrodes. In fact, it is a phenomenological lead-acid battery model which was originally proposed in [22]. The difference of developed model with model of [22] is that the effects of SOC and T on the battery model's internal impedance have been included, which is shown in (a). Therefore, the battery internal loss and the $Coulomb_{used}$ can be derived from the developed battery model under certain SOC and T. The detail and validity of this model has been presented in [23-24]. The LiFePO4 battery

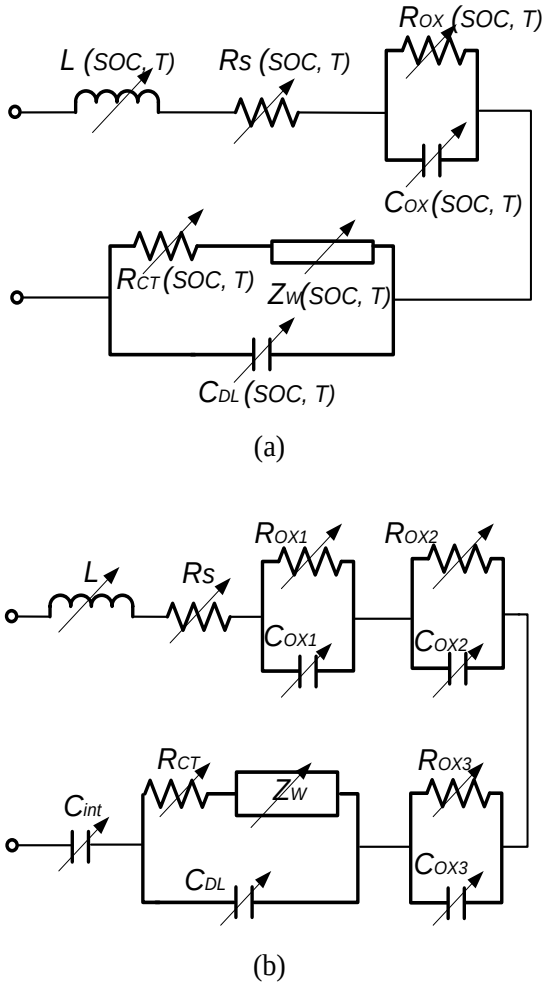

Fig. 9. Developed battery equivalent circuit model: (a) lead-acid battery model; and (b) LiFePO4 battery model.

model as a function of SOC and T has been derived and discussed in detail in [11], [25], which is presented in Fig. 9(b) for comparison.

The lifetime of lead-acid battery and LiFePO4 battery is compared in Fig. 10(a), respectively. Compared to LiFePO4 battery, lead-acid battery is cheaper but its lifespan is considerably shorter. Therefore, the levelized cost of the lead-acid battery is significantly higher than that of the LiFePO4 battery, which is demonstrated in Fig. 10(b). Consequently, Fig. 11 illustrates that the revenue change of lead-acid battery is always negative under all E_B and *d*, which means that the targeted utility cannot gain any profit if the lead-acid battery is applied. Nonetheless, based on the analysis results, it is clear that *d* = 50% is the most effective EMS design when E_B is smaller than 4.5MWh. For the rest of E_B, *d* = 70% is the best EMS option if lead-acid battery is applied, which is different if compared with LiFePO4 battery design. Table I has summarized all the key parameters used in the simulation study.

This article has been accepted for publication in a future issue of this journal, but has not been fully edited. Content may change prior to final publication. Citation information: DOI 10.1109/TIE.2017.2721878, IEEE Transactions on Industrial Electronics

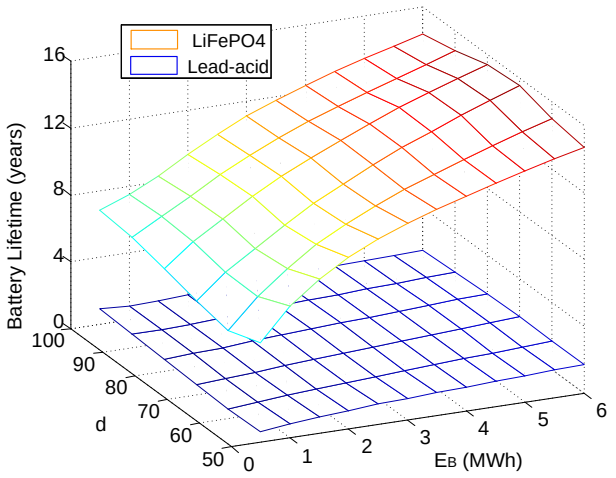

(a)

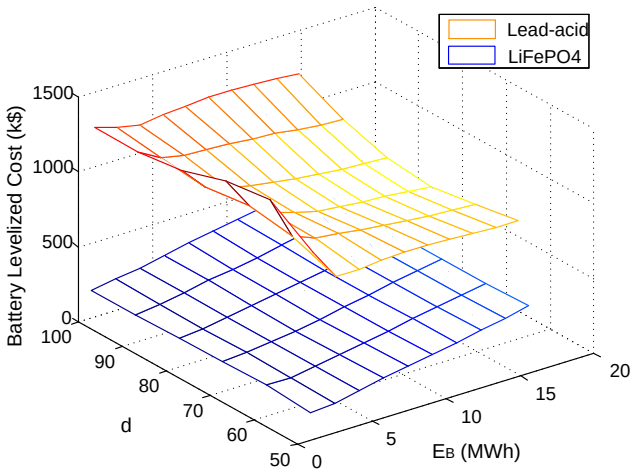

(b)

Fig. 10 Comparison of lead-acid battery and LiFePO4 battery: (a) lifetime; and (b) levelized cost.

Table I Key parameters adopted in the simulation

Parameters	Symbol	Value	Reference
Unit levelized annual cost of gas combustion turbine	LC_{CT}	120$/kW-y	PJM Interconnection [19]
Unit PCS cost	C_{PCS}	400$/kW	SANDIA [20]
Installation cost factor	$CF_{install}$	5%	EPRI [21]
Interest rate	N	0.04	NREL [26]
LiFePO4 battery unit cost	C_W	300$/kWh	California Energy Commission [27]
Lead-acid battery unit cost	C_W	100$/kWh	Ultralife [28]
Electricity price	EP	0.60$/kWh	New Solar Investment [29]

V. Conclusion

Currently battery sizing for utility scale PV plant is mainly focused on system requirement without economic analysis. This paper proposed a novel battery size design method to consider both system requirement and economic analysis. Further contributions of this paper are listed as follows:

1) The EMS affects the battery sizing and corresponding economic analysis, which has been taken into account in the proposed design. Therefore, the EMS design parameter d is derived with battery sizing to gain economic benefits using the method of exhaustion.
2) A lead-acid battery lifetime model is used for comparison which includes the effects of SOC and T on the battery model's internal impedance. Therefore, the avenue of lead-acid battery-based design can be derived and compared with that of Lithium-ion battery. The research finds that based on current battery price, the annual benefit by using lead-acid battery is negative. However, the usage of Lithium-ion battery can improve the benefit by 6%.
3) The 1-minute interval PV plant output with load data from one utility company in Florida and the actual temperature data are applied to derive realistic results.

The proposed method can also be applied to utility power systems with large-scale PV units if battery storage is used to achieve other functions including spinning reserve and frequency regulation with some modifications.

References

[1] Global Market Outlook for Photovoltaics 2013-2017 [Online]. Available: http://www.epia.org/fileadmin/user_upload/Publications/GMO_2013_-_Final_PDF.pdf

[2] Y. Noro, S. Naoi, K. Toba, M. Kimura, T. Minegishi, M. Shimizu, S. Aoki, and Y. Okuda, "Power fluctuation suppression system for large scale PV," *2012 IEEE PES Transmission and Distribution Conference and Exposition (T&D)*, vol., no., pp.1-6, May 2012.

[3] Fundamental drivers of the cost and price of operating reserves [online]. Available: http://www.nrel.gov/docs/fy13osti/58491.pdf

[4] A. Nagarajan and R. Ayyanar, "Design and Strategy for the Deployment of Energy Storage Systems in a Distribution Feeder With Penetration of Renewable Resources," in *IEEE Transactions on Sustainable Energy*, vol. 6, no. 3, pp. 1085-1092, July 2015.

[5] L. Xiangjun, H. Dong, and L. Xiaokang, "Battery Energy Storage Station (BESS)-Based Smoothing Control of Photovoltaic (PV) and Wind Power Generation Fluctuations," *IEEE Transactions on Sustainable Energy*, vol. 4, no. 2, pp. 464-473, April 2013.

[6] H. Beltran, E. Bilbao, E. Belenguer, I. Etxeberria-Otadui, and P. Rodriguez, "Evaluation of Storage Energy Requirements for Constant Production in PV Power Plants," *IEEE Transactions on Industrial Electronics*, vol. 60, no. 3, pp. 1225-1234, March 2013.

[7] R. Yu, J. Kleissl, and S. Martinez, "Storage Size Determination for Grid-Connected Photovoltaic Systems," *IEEE Transactions on Sustainable Energy*, vol. 4, no. 1, pp. 68-81, Jan. 2013.

[8] C. Venu, Y. Riffonneau, S. Bacha, and Y. Baghzouz, "Battery storage system sizing in distribution feeders with distributed photovoltaic systems," *Power Tech, 2009 IEEE Bucharest*, pp.1-5, June 2009.

[9] B. Verhelst, C. Debruyne, J. Vanalme, J. Desmet, J. Capelle, and L. Vandevelde, "Economic evaluation of the influence of overvoltages and

the integration of small storage capacity in residential PV-installations," *2011 2nd IEEE PES International Conference and Exhibition on Innovative Smart Grid Technologies (ISGT Europe)*, pp.1-6 2011.
[10] A. Oudalov, R. Cherkaoui, and A. Beguin. "Sizing and optimal operation of battery energy storage system for peak shaving application," *Power Tech, 2007 IEEE Lausanne*, pp. 621-625, July 2007.
[11] Y. Yang, H. Li, A. Aichhorn, J. Zheng, and M. Greenleaf, "Sizing Strategy of Distributed Battery Storage System With High Penetration of Photovoltaic for Voltage Regulation and Peak Load Shaving," *IEEE Transaction on Smart Grid*, vol. 5, no. 2, pp. 982-991, 2014.
[12] H. Beltran, E. Perez, N. Aparicio, and P. Rodriguez, "Daily solar energy estimation for minimizing energy storage requirements in PV power plants," *IEEE Transactions on Sustainable Energy*, vol. 4, no. 2, pp. 474-481, April 2013.
[13] Y. Riffonneau, S. Bacha, F. Barruel, and S. Ploix, "Optimal Power Flow Management for Grid Connected PV Systems with Batteries," *IEEE Trans. Sustainable Energy*, vol.2, no.3, pp.309-320, July 2011.
[14] C. L. Nge, O. M. Midtgard, L. Norum, "PV with battery in smart grid paradigm: Price-based energy management system," in *38th IEEE Photovoltaic Specialists Conference (PVSC)*, pp. 575-579, June 2012.
[15] A. Saez-de-Ibarra, A. Milo, H. Gaztañaga, V. Debusschere and S. Bacha, "Co-Optimization of Storage System Sizing and Control Strategy for Intelligent Photovoltaic Power Plants Market Integration," in *IEEE Transactions on Sustainable Energy*, vol. 7, no. 4, pp. 1749-1761, Oct. 2016
[16] [Online]. Available: http://www.a123systems.com
[17] A. Farman, "Erstellen eines messtechnisch gestützten Modells zur Berechnung der kalendarischen Alterung von LiFePO4-Batterien," Hochschule München, Sept. 2010.
[18] R. Johnson, L. Johnson, L. Nelson, C. Lenox and J. Stein, "Methods of integrating a high penetration photovoltaic power plant into a micro grid," *Photovoltaic Specialists Conference (PVSC), 2010 35th IEEE*, Honolulu, HI, 2010, pp. 000289-000294.
[19] HILL, CH2M. "Cost of New Entry Estimates for Combustion-Turbine and Combined-Cycle Plants in PJM," 2011.
[20] S. M. Schoenung, and W. V. Hassenzahl, "Long-vs. Short-Term Energy Storage Technologies Analysis. A Life-Cycle Cost Study. A Study for the DOE Energy Storage Systems Program," Sandia National Laboratories, 2003.
[21] D. Raslter, A. Akhil, D. Gauntlett, and E. Cutter, "Energy Storage System Costs 2011 Update Executive Summary," EPRI, 2012, [Online]. Available: http://www.eosenergystorage.com/documents/EPRI-Energy-Storage-Webcast-to-Suppliers.pdf
[22] P. Mauracher and E. Karden, "Dynamic modelling of lead/acid batteries using impedance spectroscopy for parameter identification," *Journal of Power Sources*, vol. 67, pp. 69-84, Aug. 1997.
[23] A. Aichhorn, M. Greenleaf, H. Li, and J. Zheng, "A cost effective battery sizing strategy based on a detailed battery lifetime model and an economic energy management strategy," *2012 IEEE Power and Energy Society General Meeting*, pp. 1-8, July 2012.
[24] M. Greenleaf, "Physical based modeling and simulation of LiFePO4 secondary batteries", thesis, Dept.ECE., Florida State Univ. Tallahassee, 2010.
[25] M. Greenleaf, H. Li and J. P. Zheng, "Modeling of LixFePO4 Cathode Li-Ion Batteries Using Linear Electrical Circuit Model," *IEEE Transactions on Sustainable Energy*, vol. 4, pp. 1-6, 2013.
[26] [Online]. Available: http://www.nrel.gov/analysis/tech_lcoe.html
[27] [Online]. Available: http://www.energy.ca.gov/2015publications/CEC-500-2015-020/CEC-500-2015-020.pdf
[28] [Online]. Available: ultralifecorporation.com/download/275/

Ye Yang received the B.S. degree in information engineering from Tianjin University, Tianjin, China, in 2008, and the M.S. degree in electrical engineering from Texas Tech University, Lubbock, TX, USA, in 2010. He received the Ph.D. degree from Florida State University, Tallahassee, FL, USA, in 2014. He is currently with the National Institute of Clean-and-Low-Carbon Energy, Beijing, China.

Qing Ye (S'14) received the B.S. and M.S. in Electrical Engineering from Huazhong University of Science and Technology, China in 2010 and 2013, respectively. He is currently working toward the Ph.D. degree in the Center for Advanced Power Systems, Florida State University, Tallahassee, FL.

His research interests include the smart grid, energy storage and renewable energy applications.

Leonard J. Tung received his Ph.D. degree in electrical engineering from Texas Tech University in 1977. He was at University of Texas at El Paso from 1978 to 1979. He was at Old Dominion University in Norfolk, VA, from 1979 to1983. He joined Florida State University in 1984. His research interest is control system and design.

Michael Greenleaf (M'06) received the B.S., M.S. and Ph.D degree in electrical engineering at Florida State University, Tallahassee, FL, USA, in 2008, 2010, 2014, respectively. He is currently with U.S. Nuclear Regulatory Commission, Atlanta, Georgia, USA.

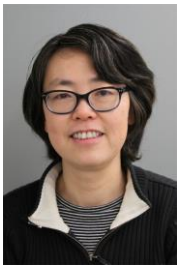

Hui Li (S'97–M'00–SM'01) received the B.S. and M.S. degrees in electrical engineering from Huazhong University of Science and Technology, Huazhong, China, in 1992 and 1995, respectively. She received the Ph.D. degree in Electrical Engineering from the University of Tennessee, Knoxville, TN, USA, in 2000.

She is currently a Professor in the Electrical and Computer Engineering Department at the Florida A&M University—Florida State University College of Engineering, Tallahassee, FL, USA. Her research interests include PV converters, energy storage applications and smart grid.